Received: 11 September 2023 | Accepted: 13 November 2023

DOI: 10.1111/jpy.13411

RESEARCH ARTICLE

Description of six new cyanobacterial species from soil biocrusts on San Nicolas Island, California, in three genera previously restricted to Brazil

Brian M. Jusko[1] | **Jeffrey R. Johansen**[1,2]

[1]Department of Biology, John Carroll University, University Heights, Ohio, USA

[2]Department of Botany, Faculty of Science, University of South Bohemia, České Budějovice, Czech Republic

Correspondence
Brian M. Jusko, Department of Biology, John Carroll University, University Heights, OH 44118, USA.
Email: bjusko18@jcu.edu

Funding information
U.S. Navy, Grant/Award Number: N62473-21-2-0002

Editor: J.L. Collier

Abstract

As the taxonomic knowledge of cyanobacteria from terrestrial environments increases, it remains important to analyze biodiversity in areas that have been understudied to fully understand global and endemic diversity. This study was completed as part of a larger algal biodiversity study of the soil biocrusts of San Nicholas Island, California, USA. Among the taxa isolated were several new species in three genera (*Atlanticothrix*, *Pycnacronema*, and *Konicacronema*) which were described from, and previously restricted to, Brazil. New taxa are described herein using a polyphasic approach to cyanobacterial taxonomy that considers morphological, molecular, ecological, and biogeographical factors. Morphological data corroborated by molecular analysis including sequencing of the 16S rRNA gene, and the associated 16S–23S ITS rRNA region was used to delineate three new species of *Atlanticothrix*, two species of *Pycnacronema*, and one species of *Konicacronema.* The overlap of genera from San Nicolas Island and Brazil suggests that cyanobacterial genera may be widely distributed across global hemispheres, whereas the presence of distinct lineages may indicate that this is not true at the species level. Our data suggest that based upon global wind patterns, cyanobacteria in both Northern and Southern hemispheres of the Americas may have a more recent common ancestor in Northern Africa, but this common ancestry is distant enough that speciation has occurred since transatlantic dispersal.

KEYWORDS
Atlanticothrix, biological soil crusts, Brazil, cyanobacteria, *Konicacronema*, polyphasic approach, *Pycnacronema*, San Nicolas Island, species distribution, taxonomy

INTRODUCTION

Although soils hold a significant portion of global microbial diversity, they are vastly understudied taxonomically. In particular, the biodiversity present in soils of arid environments is not well understood. In these areas, biological soil crusts (BSCs) consisting of a consortium of microorganisms (cyanobacteria, green algae, lichens, fungi, and heterotrophic bacteria) form on the top layer of the soil surface (Belnap, 2003; Weber et al., 2022). These BSCs are ecologically significant for their ability to prevent erosion, to prevent desiccation, and to increase

Abbreviations: BI, Bayesian Inference; BSCs, biological soil crusts; DIC, differential interference contrast; GTR, general time reversible; ITS, internal transcribed spacer; MCMC, Markov chain Monte Carlo; ML, maximum likelihood; MP, maximum parsimony; PCR, polymerase chain reaction; PRSF, potential Scale Reduction Factor; RNA, ribonucleic acid; SNI, San Nicolas Island.

soil fertility via atmospheric fixation of carbon and nitrogen (Evans & Johansen, 1999; Harper & Marble, 1989; Jeffries et al., 1993; Kleiner & Harper, 1972; Pietrasiak et al., 2013; West, 1990). Among the most significant and abundant members of these biocrusts are cyanobacteria, which can bind soil particles and can increase biogeochemical cycling in an otherwise limited environment (Evans & Johansen, 1999). Studies have shown cyanobacteria present in BSCs to be diverse, and new taxa continue to be described from studies in these environments (Baldarelli et al., 2022; Becerra-Absalón et al., 2018, 2020; Flechtner et al., 2002; Jung et al., 2020; Mesfin et al., 2020; Pietrasiak et al., 2019, 2021; Řeháková et al., 2007).

As taxonomic knowledge of cyanobacteria increases, species representing genera previously thought to be geographically restricted have been found in distant locations (Brown et al., 2021; Hentschke et al., 2017; Kaštovský et al., 2023; Osorio-Santos et al., 2014; Shalygin et al., 2020). While some terrestrial cyanobacterial species such as *Microcoleus vaginatus* are known to have widespread distributions (Dvořák et al., 2012), most subaerial and terrestrial species have been oberserved only in relatively isolated areas (Mühlsteinová et al., 2014; Sherwood et al., 2015). It was previously hypothesized that microbial organisms might have cosmopolitan distributions (Bass-Becking, 1934), but this hypothesis has been challenged in the absence of human vectoring (Hentschke et al., 2017). Genera on the other hand can often be found in ecologically different and geographically isolated environments (Jung et al., 2020). Although the criteria that group species into the taxonomic category "genus" are subjective, the evolutionary relationships among lineages are objective. Genetic relatedness suggests a more recent common ancestor, and the distribution of closely related species across geographical space raises questions about the speed and ease with which terrestrial algal taxa relocate and diversify.

San Nicholas Island (SNI) is geographically isolated from mainland North America, being 98 km off the coast of Santa Barbara, California, USA, and is part of an eight-island archipelago known as the Channel Islands. Several of the Channel Islands comprise a national park; however, SNI serves as a Naval Base for the US Navy with public access restricted, leaving it relatively undisturbed compared with other habitats in the western United States. San Nicholas Island experiences a semi-arid climate, receiving about 200 mm of precipitation per year, albeit with relatively high humidity relative to other arid systems due to sea sprays from the Pacific Ocean. Although the island is small and primarily composed of limestone (58.9 km^2), it has significant topographic and geological variation. The northwest side of the island is characterized by stabilized sand dunes and gentle slope, while the south side of the island is gypsiferous with steep cliffs. Also found on the island are natural springs, salty chemical crusts, and lichenized soil crusts at various stages of development. Due to the restricted access, only one previous biocrust study has been done on the island (Flechtner et al., 2008). In that study, 56 species of algae were observed and characterized, with seven new species of cyanobacteria and two new species of chlorophytes being described based on morphological data alone. San Nicolas Island is consequently an ideal site for a new taxonomic study integrating genetic data.

In this paper, three new species of *Atlanticothrix*, two new species of *Pycnacronema*, and one new species of *Konicacronema* are described utilizing a polyphasic approach (Mühlsteinová et al., 2014) that considers morphological, genetic, and ecological characteristics. *Atlanticothrix* is a genus in the family Nostocales with one currently described species, *A. silvestris* (Alvarenga et al., 2021). *Pycnacronema* and *Konicacronema* are large filamentous genera recently moved to Wilmottiaceae and Konicacronemataceae, respectively (Strunecký & Ivanova, 2023). There are currently nine recognized species of *Pycnacronema* and one species of *Konicacronema*, *K. caatingense*. Currently, most species representing these three genera have been described from terrestrial or aerial environments in Brazil (Alvarenga et al., 2021; Machado de Lima & Branco, 2020; Martins et al., 2018). One aquatic species of *Pycnacronema*, *P. lacustrum*, was just described from a lake in the Azores (Luz et al., 2023). However, multiple strains representing new species have been found on SNI. The overlap among these genera (but not species) between North and South America may shed light on cyanobacterial distributions at the genus level.

METHODS

Field collection

A total of 36 soil samples, most with a biocrust surface, were collected from sites on SNI (Figure 1) with one additional reference sample from nearby Santa Barbara Island (SBI). Samples SBI and SNI-TA1 through SNI-TA5 were collected on 11 February 2021 and samples SNI-TA6 through SNI-TA36 were collected on 25 May 2021. Samples were collected with a metal spoon and transferred into plastic bags for storage and shipping. Example images showing the diversity of soil crust types can be found in the Figure S1 in the Supporting Information.

Isolation and culture

From each sample, 1.0 g subsamples were separated from larger fragments of crusted soil, diluted in

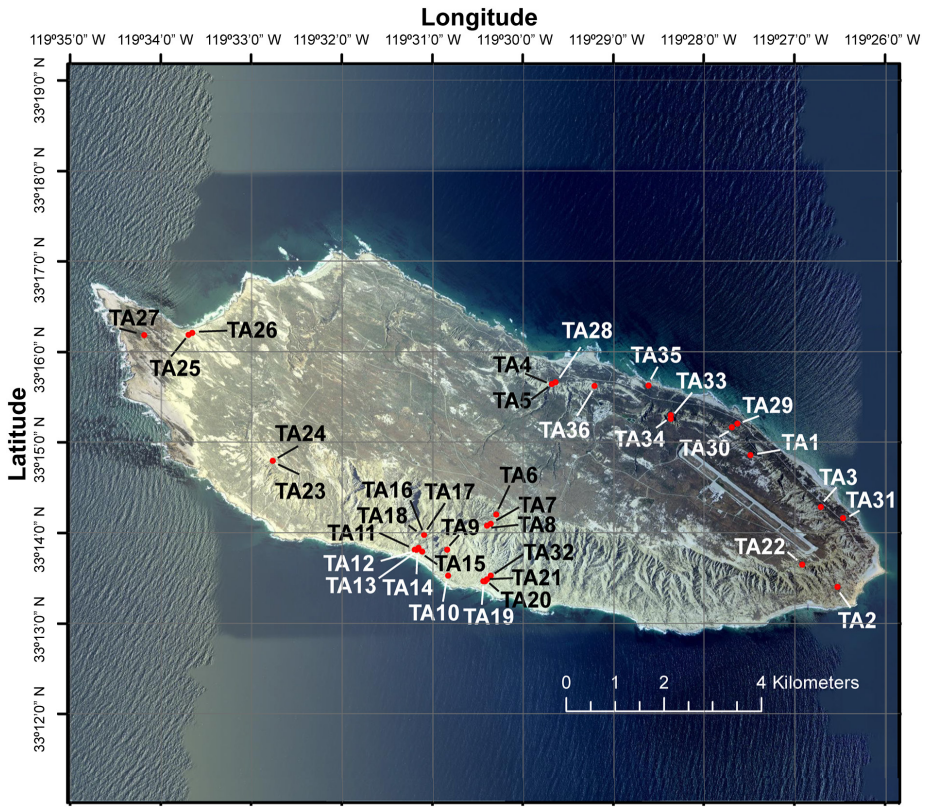

FIGURE 1 A map of San Nicolas Island. Study sites are superimposed on the map. (Color figure can be viewed at wileyonlinelibrary.com). [Color figure can be viewed at wileyonlinelibrary.com]

Erlenmeyer flasks with 100 mL sterile liquid Z8 media (Carmichael, 1986) and agitated for 30 min on a rotary shaker to release the cyanobacteria from the soil matrix. Enrichment plates of agar-solidified Z8 were inoculated with 0.1 mL of the soil solution from each sampling site with three replicates. Plates were sealed with Parafilm (Bemis Company, Inc., Neenah, WI) and placed under a 12 h:12 h light:dark cycle at 20°C until macroscopic algal colonies were visible (about 5 weeks). Uniagal cultures were obtained by picking well-isolated colonies under an Olympus SZ40 stereoscope (Olympus Corporation, Tokyo) into capped test tubes containing 5.0 mL sterile liquid Z8 media and returned to the 12 h:12 h light:dark cycle until significant growth was observed. Developed cultures were transferred to sterile agar-solidified Z8 slants. Strains were named for site (e.g., SNI-TA17) and person isolating the culture (e.g., SNI-TA17-BJ3, BJ3 for third isolate Brian Jusko isolated from sample SNI-TA17). Cultures are maintained in the Algal Culture Collection at John Carroll University. Herbarium vouchers of immobilized, air-dried material (including holotypes, isotypes, and paratypes) were deposited in the Clifton Smith Herbarium at the Santa Barbara Botanic Garden, Santa Barbara, California, USA.

Morphological characterization

Strains were observed, photographed, and characterized morphologically using an Olympus BH-2 microscope equipped with Nomarski DIC optics and cellSens software (Olympus Corporation, Tokyo). A minimum of 20 photographs were taken of each strain with care given to capture all specialized cell types and life-cycle stages. Length and width measurements were taken for vegetative cells, filament width, apical cells, and heterocytes and akinetes when applicable. Other relevant morphological features such as cell shapes and color were noted. *Atlanticothrix* strains were later transferred to nitrogen-free Z8 medium to promote further heterocyte growth and were again photographed.

To determine if *Atlanticothrix* strains could be separated in species based on cell size, a principal component analysis was performed using mean measurements (vegetative cell, akinetes, heterocytes, and apical cell) and length-width ratios obtained from *Atlanticothrix* strains in R (v. 4.2.1). To obtain each average measurement value, 30 individual length and width measurements were taken for each cell type, averaged, and assigned to the respective strain.

Molecular characterization

Genomic DNA was extracted from strains using Qiagen DNeasy Powersoil Pro Kits (Qiagen, Hilden, Germany) following the manufacturer's protocol and eluted in 50 μL of elution buffer. Polymerase chain reaction (PCR) was used to amplify the 16S rRNA gene and the 16S–23S rRNA internal transcribed spacer (ITS) region using primers VRF1R and VRF2F (Flechtner et al., 2002; adopted from Wilmotte et al., 1993). The reaction mixture containing 1 μL of each primer at 0.01 mM concentration was combined with 12.5 μL of LongAmp™ Taq 2x Master Mix (NEB, Ipswitch MA), 1 μL template DNA (50 ng · mL^{-1}), and 9.5 μL nuclease free water. This PCR mix was subjected to 35 cycles of denaturing (94°C for 45 s), annealing (at 57°C for 45 s), an extension (at 72°C for 135 s), and a final extension (at 72°C for 5 min). Polymerase chain reaction products were inserted into the *lac*Z gene of plasmid pSC-A-amp.kan and cloned into StrataClone (Agilent, Santa Clara, CA) competent *Escherichia coli* cells via heat shock following the manufacturer's protocol. *Escherichia coli* cells were plated on agar-solidified LB-ampicillin plates with 40 μL X-Gal, and three properly transformed colonies were picked via blue-white screening. Plasmid DNA was isolated with Qiagen QIAprep Miniprep kits following the manufacturer's protocol. Insertions were confirmed by *Eco*R1 restriction enzyme digest followed by visualization on 1% TBE agarose gels. Two or three clones of each strain were sent to Functional Biosciences, Inc (Madison, WI, USA) for Sanger sequencing. Primers M13 forward and M13 reverse and internal primers VRF5 (5′-TGT ACA CAC CGG CCC GTC-3′), VRF7 (5′-AAT GGG ATT AGA TAC CCC AGT AGT C-3′), and VFR8 (5′-AAG GAG GTG ATC CAG CCA CA-3′; Nübel et al., 1997; Wilmotte et al., 1993) were used to obtain partial overlapping sequences. Sequences were error proofed using Chromas software (v. 2.6.6) and assembled into contigs by alignment with ClustalW (Larkin et al., 2007). When possible, two or three clones were used to construct consensus sequences.

Phylogenetic analyses

The 16S rRNA gene (a partial sequence of 1162–1171 nucleotides) was subjected to analysis by both Bayesian inference (BI) and maximum likelihood (ML) analyses using the CIPRES Science Gateway (Miller et al., 2010) to obtain posterior probability and bootstrap support values for each node in the tree. Bayesian inference analyses were performed using MrBayes on XSEDE 3.2.6 (Ronquist et al., 2012), and ML analyses were performed using RAxML-HPC2 on XSESE 8.2.10 (Stamatakis, 2014). In both cases, the GTR + I + G evolutionary model was used. The BI analysis was run for 80 million generations with the first 25% of samples discarded as burn-in. The ML analysis was run on the same alignments with 1000 bootstrap iterations. 16S rRNA gene analyses were performed at the family or order level with several representatives from each related genus for which sequences were available in GenBank, to produce robust phylogenetic trees. Posterior probability and bootstrap support values (from BI and ML analyses, respectively) were superimposed on the phylogenetic trees at nodes. The BI analysis had a mean estimated sample size (ESS) exceeding 2900 (range: 2919–13,027) for all parameters, significantly higher than the average of 100 accepted as sufficient (Drummond et al., 2006). The average standard deviation of split frequencies was ≤0.01. The potential scale reduction factor (PSRF) value for all parameters in the BI analyses was 1.00, indicating that the convergence of the MCMC chains was achieved (Gelman & Rubin, 1992). Internal transcribed spacer rRNA region phylogenetic analyses were performed using alignments of species within a genus (565 nucleotides long for *Atlanticothrix*, 491 nucleotides long for *Pycacronema*). These alignments were used to run BI analyses as well as maximum parsimony (MP) analyses to determine relationships among closely related strains. Maximum parsimony analyses were run in PAUP using the parameters GAP = NEWSTATE, NREPS = 10,000, MULTREES = YES, SWAP = TBR, and STEEPEST = NO. The BI analysis used the GTR + G + I evolutionary model with two data partitions; one for the DNA sequences and one for coding indels as standard data (1 = nucleotides, 0 = indel, and ? = missing). Bootstrap values from the MP analyses were mapped onto shared nodes of the BI tree. Phylogenetic trees were visualized with Fig Tree (Rambaut, 2009) and post-edited in Adobe Illustrator (v. 26.4.1; Adobe Systems, San Jose, California).

Percent identities among 16S rRNA gene sequences and percent dissimilarities among 16S-23S ITS rRNA regions were determined using the SHOWDIST command in PAUP (Swofford, 1998). Hypothetical ITS rRNA region secondary structures for the D1-D1', Box-B, and V2 and V3 helices were identified based on conserved basal clamps. Location of basal clamps for SNI strains were determined by creating multiple alignments of closely related taxa with ClustalW (Larkin et al., 2007) and using existing taxa with known helix locations as a guideline. Secondary structures were determined via Mfold (Zuker, 2003) on the UNAFold Web Server (http://www.unafold.org). Drawing mode was set to untangle with loop fix and all other settings were set to default. Secondary structures derived from Mfold were post-edited in Adobe Illustrator. Lines connecting bases were used to represent canonical pairings and dots were used to represent noncanonical U-G pairings.

RESULTS

Genus *Atlanticothrix*

Atlanticothrix crispata Jusko et J.R.Johans. sp. nov. Figure 2l–q

Description: Colonies on agar soft, mucilaginous, not shiny, becoming mounded, blue-green, purplish, or brownish depending on stage of life cycle. Filaments uniseriate, with thin diffluent mucilage, not forming *Nostoc*-like colonies, often with mucilage not evident, consisting of vegetative cells early in life cycle, but soon producing long continuous series of purplish to brownish akinetes. Trichomes of vegetative cells thin, with conical vegetative cells at ends, or with bluntly conical and flame-shaped terminal heterocysts, constricted at crosswalls, blue-green or purple in color when composed of vegetative cells, brown in color when composed of maturing-to-mature akinetes, 1.8–3.4 μm wide (2.6 μm average). Vegetative cells cylindrical or barrel-shaped, not moniliform, sometimes slightly constricted in mid-cell, mostly non-granular, with some being minutely granular, 1.9–4.9 μm long (2.9 μm average). Heterocytes mostly terminal with a single polar nodule, rounded, becoming elongated and bluntly conical, 2.0–3.1 μm wide, 3.0–5.3 μm long, rare intercalary heterocytes oval, with paired polar nodules 2.0–4.0 μm wide,

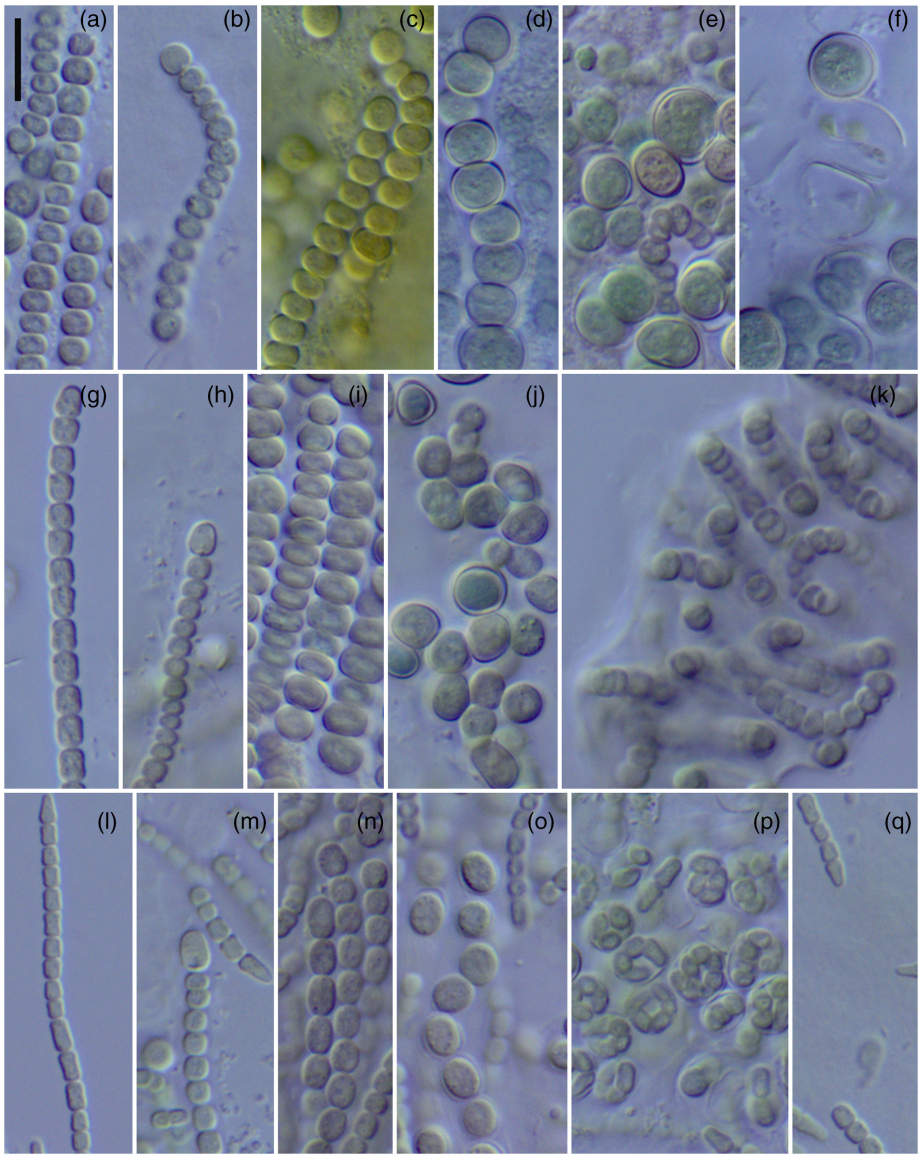

FIGURE 2 Images showing diagnostic morphological features for each *Atlanticothrix* species (Scale bar = 10 μm, applies to the entire figure). All photos are 1000× magnification. (a–f) *Atlanticothrix testacea* SNI-TA4-BJ2. (g–k) *Atlanticothrix nostocoides* (g, j: SNI-TA5-JJ1, h, i: SNI-TA1-JJ4, k: SNI-TA5-JJ3) note diagnostic *Nostoc*-like colonies in (k). (l–q) *Atlanticothrix crispata* (m: SNI-TA23-BJ41, n, p, q: SNI-TA26-BJ1, m, o: SNI-TA26-BJ7) note diagnostic curled hormogonia in P. (Color figure can be viewed at wileyonlinelibrary.com). [Color figure can be viewed at wileyonlinelibrary.com]

2.4–4.4 μm long. Akinetes develop continuously from vegetative cells by increase in both length and width, when mature having thickened outer wall, before germination transitioning from brown to blue-green in color, revealing multiple vegetative cells immediately before germination when akinete can become enlarged to accommodate curled germinating trichomes, 3.2–7.4 μm wide, 3.1–7.4 μm long. Discarded cell walls of akinetes persist following release of hormogonia.

Holotype here designated: SBBG238511! Dried immobilized material prepared from the reference strain, SNI-TA26-BJ1.

Isotype here designated: SBBG238512! Dried immobilized material prepared from the strain, SNI-TA26-BJ7.

Paratypes here designated: SBBG238508! SBBG238509! SBBG238510! Dried immobilized material prepared from strains, SNI-TA18-ML7, SNI-TA23-BJ35, SBI-TA23-BJ41, respectively.

Type locality: BSC from sample SNI-TA26 (Figure S1C), San Nicolas Island, Ventura County, California, 33.27037, –119.56095.

Etymology: L. *crispatus* = curly, referring to the tightly curled hormogonia produced in akinetes before germination.

Altanticothrix nostocoides Jusko et J.R.Johans. sp. nov. Figure 2g–k

Description: Colonies on agar soft, mucilaginous, somewhat shiny, becoming mounded, blue-green, purplish, or brown depending on stage of life cycle. Filaments uniseriate, with thin diffluent mucilage, occasionally with mucilage not evident, consisting of vegetative cells early in life cycle, but soon producing long continuous series of compressed blue-green to purplish brown akinetes. Filaments often form large *Nostoc*-like colonies with evident diffluent mucilage. Trichomes of vegetative cells thin, bluntly conical apical cells or bluntly flame-shaped heterocytes at one or both ends, constricted at crosswalls, blue-green to purplish in color, blue-green or purplish or brownish when akinetes develop, 2.2–4.4 μm wide. Vegetative cells barrel-shaped, occasionally minutely granular, 2.0–4.4 μm long. Heterocytes mostly terminal with a single polar nodule, bluntly rounded to bluntly flame-shaped, 2.4–4.2 μm wide, 2.4–5.2 μm long. Rare intercalary heterocytes oval with paired polar nodules, 3.6–3.8 μm wide, 3.6–5.2 μm long. Akinetes develop continuously from vegetative cells by increase in length and width, when mature having a thickened outer wall, forming in long continuous compressed series before dissociating at maturity, becoming blue-green before germination, revealing multiple vegetative cells immediately before germination when akinetes become enlarged to accommodate germinating trichomes, 3.6–7.6 μm wide, 2.6–7.4 μm long. Discarded akinete cell walls persist following release of hormogonia.

Holotype here designated: SBBG238506! Dried immobilized material prepared from the reference strain, SNI-TA5-JJ3.

Isotype here designated: SBBG238505! Dried immobilized material prepared from the strain, SNI-TA5-JJ1.

Paratype here designated: SBBG238504! Dried immobilized material prepared from the strain, SNI-TA1-JJ4.

Type locality: Uncrusted soil sample SNI-TA5 (Figure S1B), San Nicolas Island, Ventura County, California, 33.26087, –119.49422.

Etymology: L. *nostocoides* = *Nostoc*-like, so named because this is the only species in the genus observed thus far that can produce *Nostoc*-like mucilaginous colonies.

Atlanticothrix testacea Jusko et J.R.Johans. sp. nov. Figure 2a–f

Colonies on agar soft, mucilaginous, shiny when composed of vegetative cells and not shiny when akinetes develop, becoming mounded, shifting from blue-green to golden brown as vegetative cells become akinetes. Filaments uniseriate, with evident diffluent mucilage, often with mucilage absent, consisting of vegetative cells early in life cycle, but soon producing long continuous series of compressed blue-green to golden brown akinetes. Trichomes of vegetative cells thin, with rounded vegetative cells at ends, or with rounded or bluntly flame-shaped heterocytes at one or both ends, constricted at crosswalls, blue-green or purplish in color when consisting of vegetative cells, purplish to golden brown in color when composed of maturing-to-mature akinetes, 2.2–4.0 μm wide. Vegetative cells constricted to moniliform or barrel-shaped, mostly non-granular but occasionally minutely granular, 1.6–3.6 μm long. Heterocytes mostly terminal with a single polar nodule, rounded or bluntly flame-shaped, 2.8–4.3 μm wide and 2.4–4.4 μm long, rare intercalary heterocytes rounded to oval, with paired polar nodules, 4.8 μm wide and 3.6 μm long. Akinetes develop continuously from vegetative cells by increase in length and width, when mature having a thickened outer wall, before germination transitioning from golden brown to blue-green, revealing multiple vegetative cells immediately before germination when akinete can become enlarged to accommodate germinating trichomes, 4.2–8.0 μm wide, 2.8–7.2 μm long. Discarded cell walls of akinetes persist following release of hormogonia.

Holotype here designated: SBBG238507! Dried immobilized material prepared from the reference strain, SNI-TA4-BJ2.

Type locality: Moss and cyanobacterial biocrust from sample SNI-TA4, San Nicolas Island, Ventura County, California, 33.26087, –119.49422.

Etymology: L. *testaceus* = brownish yellow, named for the golden-brown color of the mature akinetes.

Phylogenetic analyses

The 16S rRNA gene analysis (Figure 3) performed with all SNI *Atlanticothrix* strains and all *A. silvestris* strains formed a well-supported (0.99 BI posterior probability, 77 ML bootstrap support) monophyletic generic clade sister to *Roholtiella*. The *A. silvestris* strains formed a monophyletic clade within the genus with a posterior probability of 0.96 suggesting that the Brazilian strains form a species that is a different lineage from all SNI strains. The 16S rRNA gene analysis at the species level among the SNI strains was, however, uninformative. All *Atlanticothrix* strains are >98.7% similar in 16S rRNA gene sequences (Table 1), and the BI/ML analyses were unable to clearly group together SNI strains at the species level.

Analysis of 16S–23S ITS rRNA region

The 16S–23S ITS rRNA region analysis (Figure 4) was more informative at resolving species. The ITS rRNA region phylogenetic analysis performed with available *Atlanticothrix* strains produced a tree with three well-supported (all 100% bootstrap support) species among the SNI strains. One operon of strain SNI-TA23-BJ35 fell sister to the *A. silvestris* clade, whereas the other operon fell clearly within the *A. crispata* clade. One operon of *A. crispata* SNI-TA23-BJ35 differed by 4.8% from *A. silvestris* and >9.7% from all members of the *A. crispata* clade. However, the other operon differed by <1% from *A. crispata* and 8.6% from *A. silvestris* (Table 1). Within each species with multiple strains, ITS rRNA region dissimilarity was <1% except for the operon mentioned above. Dissimilarity values above 7% are strong evidence that strains are different species, supporting our hypothesis that *A. silvestris*, *A. crispate*, and *A. nostocoides* form three distinct lineages. *Atlanticothrix testacea* had an ITS rRNA region that was only 2.3% dissimilar to *A. crispata* (Table 1), not supporting separation of the two taxa. However, both the 16S rRNA gene and ITS rRNA region phylogenies showed the two species to be distinct.

Analysis of ITS rRNA region secondary structures

Hypothetical secondary structures of conserved domains of the 16S-23S ITS rRNA region varied among each species. The D1-D1' helix (Figure S2A–C in the Supporting Information) varied only slightly with all three SNI strains (except one operon) sharing identical helices. The SNI structure varied slightly from the *Atlanticothrix silvestris* structure in the penultimate internal bulge with an additional adenine on either side and had one fewer set of paired bases before the next bulge. The SNI Box-B helices (Figure S2D–G) were all somewhat different from the *A. silvestris* structure and were six base pairs longer. The V3 helices (Figure S2H–K) were also somewhat similar among all species, although some base pair differences were observed among SNI strains and *A. silvestris* strains. The V2 structure (Figure 5) was the most informative at resolving lineages to the species level. The V2 representing *A. testacea* (Figure 5a) was very different from all other structures with one large internal bulge not observed in any other strain. The strains representing *A. nostocoides* (Figure 5b–d) had in common four internal bulges with the top and bottom bulges terminating in a noncanonical U-G pairing at one end. The *A. crispata* helices (Figure 5e,f) were the most similar to *A. silvestris* (Figure 5h,i); however, they shared in common a terminal loop sequence and an unpaired uracil three base pairs upstream of the terminal loop. One operon of SNI-TA23-BJ35 had unique V2 helix secondary structures from all other SNI and *A. silvestris* strains (Figure 5g). The V2 helix was the portion of the ITS rRNA region with the highest proportion of overall dissimilarity among strains and is the best evidence of separate lineages.

Morphological analysis

All strains were grown in identical conditions, and distinctive morphological features were observed among species. *Atlanticothrix crispata* was distinctive in the formation of curled trichomes with conical end cells inside germinating akinetes (Figure 2p). This feature was observed regularly in multiple strains of this species and never observed in strains of other species. The akinetes of this species formed in uncompressed series and were often longer than wide, which was unlike the highly compressed wider-than-long series observed in the *A. nostocoides* and *A. testacea* (Figure 2c–f,i–j,n–o). *Atlanticothrix testacea* was unique in its formation of golden brown akinetes (Figure 2c).

Strains of *Atlanticothrix nostocoides* were the only strains to exhibit formation of large distinctive *Nostoc*-like colonies (Figure 2k). Colonies with obvious diffluent mucilage formed consistently in all strains representing the species and were never observed in other species, including *A. silvestris*.

Vegetative cells and apical cells also varied among species. *Atlanticothrix crispata* often developed rounded end cells that were indistinguishable from other vegetative cells in the filament (Figure 2a). This was also the only species to develop rounded

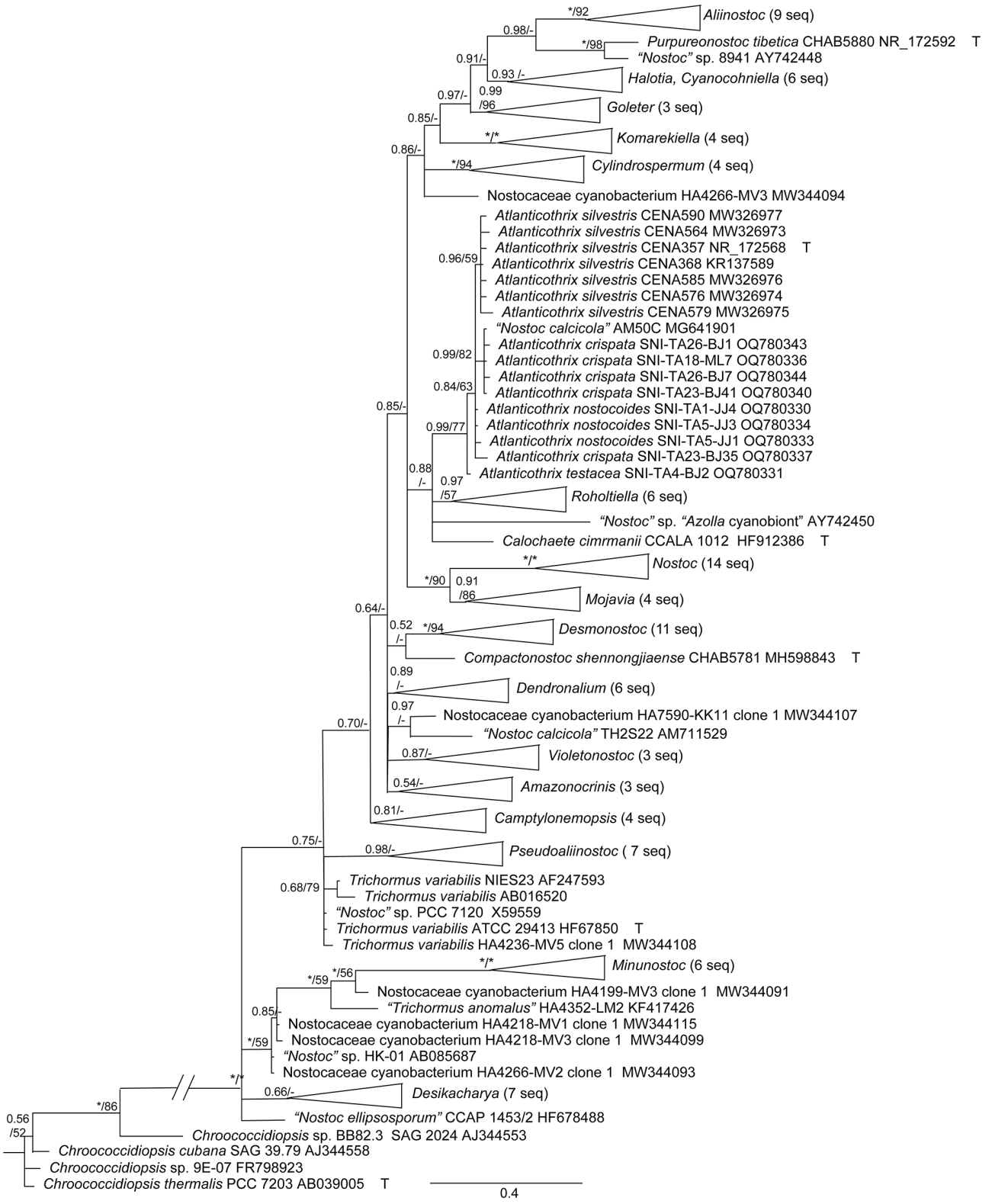

FIGURE 3 Nostocaceae Bayesian inference 16S rRNA gene phylogeny with maximum likelihood bootstrap support values added to nodes. "*" indicates full support for nodes (1.0 posterior probability or 100 bootstrap support). "-" indicates bootstrap support <50. All available *Atlanticothrix sivestris* and San Nicholas Island *Atlanticothrix* sequences were included in the analysis. The genus level *Atlanticothrix* clade had high support (0.99 BI, 77 ML), although 16S rRNA gene data were uninformative at the species level.

vegetative cells in moniliform series. In most cases, *A. nostocoides* developed bluntly conical apical cells that were longer than wide (Figure 2g). Conversely, *A. testacea* developed distinctly conical end cells coming to a fine point (Figure 2l). This type of apical cell was not observed in the other species.

TABLE 1 Percent identity of 16S rRNA gene sequences and percent dissimilarity of ITS sequences among species of *Atlanticothrix*.

	A. silvestris	*A. crispata*	*A. nostocoides*	*A. testacea*
16S rRNA percent identity				
A. silvestris	99.78			
A. crispata	99.61	99.77		
A. nostocoides	99.76	99.76	99.91	
A. testacea	99.63	99.68	99.76	100.0

	A. silvestris	*A. crispata* operon 1	*A. crispata* operon 2	*A. nostocoides*	*A. testacea*
ITS percent dissimilarity					
A. silvestris	0.22				
A. crispata, operon 1	8.60	0.19			
A. crispata operon 2	4.80	9.77	NA		
A. nostocoides	13.71	7.15	15.06	0.25	
A. testacea	9.03	2.32	10.17	6.56	0.00

Note: Infraspecific means are highlighted. The two operons of *A. crispata* are scored separately for the ITS rRNA gene region due to their high infraspecific dissimilarity.

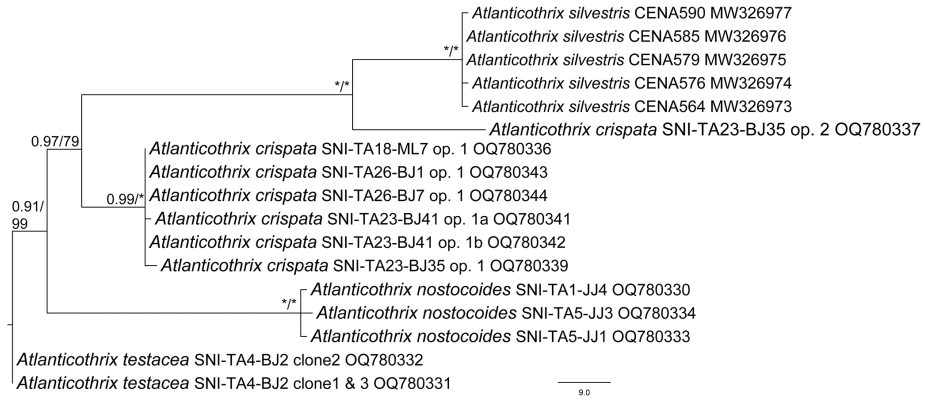

FIGURE 4 Maximum parsimony phylogenetic tree based on 16S-23S ITS rRNA region sequences. All available *Atlanticothrix silvestris* and San Nicholas Island *Atlanticothrix* sequences were used in the analysis.

There was overlap in many of the length and width measurements for each cell type among species, so a principal component analysis (PCA) was performed (Figure S3 in the Supporting Information) using mean length and width measurements for vegetative cells, apical cells, heterocytes, and akinetes as well as length-width ratios for each measurement (based on 30 measurements for each parameter). The PC1 and PC2 axes explained 54.6% and 21.3% of variation in the data, respectively, for a total of 75.9% variation explained. Vegetative cell length, width, and length-width ratio, as well as apical cell length-width ratio were the traits most strongly associated with PC1. Heterocyte width and akinete diameter were the traits most strongly associated with PC2. Heterocyte length and length-width ratio contributed to both axes. In general, strains were separated into species groups along PC1. *Atlanticothrix crispata* was isolated from all other strains in the analysis on the far left of the graph. Strains representing *A. nostocoides* formed a group in the center of the graph. *Atlanticothrix testacea* strains were the most ambiguous with two on the far right and one at both the top and bottom of the PCA plot. Although some overlap exists in cell measurements among species, the PCA along with the previously mentioned distinctive features serves as evidence that the lineages have evolved diagnosable morphological traits.

Genus Pycnacronema

Pycnacronema flechtnerae Jusko et J.R. Johans. sp. nov. Figure 6a–e

Filaments solitary or forming non-entangled bundles, without trichomes sharing common sheath, 7.0–8.2 μm wide. Sheaths firm, hyaline, thin, occasionally extending beyond trichome. Trichomes with gliding motility, minutely constricted at crosswalls, cylindrical, tapered slightly when conical apical cell present, lacking necridia, 4.6–7.0 μm wide. Cells wider than long or isodiametric, green to blue-green, with visible crosswalls,

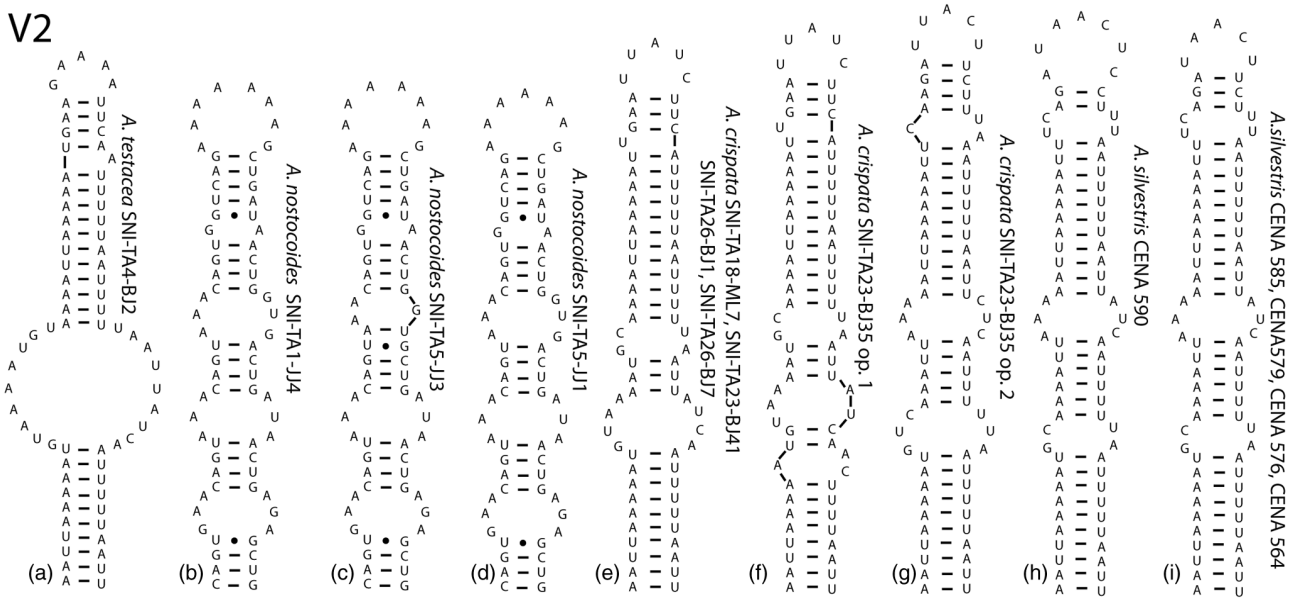

FIGURE 5 Hypothetical ITS rRNA region secondary structures for the V2 helix for all strains representing *Atlanticothrix crispata*, *A. testacea*, *A. nostocoides*, and *A. silvestris*. Representative strains for each helix are listed on the figure. (a) *A. testacea*. (b–d) *A. nostocoides*. (e–g) *A. crispata*. (h–i) *A. silvestris*.

occasionally with granular contents, with thylakoids sometimes appearing distinctively fasciculated, 2.6–5.8 μm long. Apical cells bluntly rounded when hormogonia form but becoming elongated and bluntly conical, yellow in color, 4.8–6.8 μm wide, 5.0–10.6 μm long.

Holotype here designated: SBBG238513! Dried immobilized material prepared from the reference strain, SNI-TA3-BJ5.

Type locality: Lichenized moss and algal biocrust from sample SNI-TA3, San Nicolas Island, Ventura County, California, 33.23795, –119.44460.

Etymology: Named for Valerie R. Flechtner, first author on the taxonomic study of soil algae of San Nicolas Island (Flechtner et al., 2008) and colleague and friend to the second author of this paper.

Pycnacronema aeruginosum Jusko et J.R.Johans. sp. nov. Figure 6f–k

Filaments either solitary or forming bundles of parallel filaments, without trichomes sharing a common sheath, 4.6–6.6 μm wide. Sheaths firm, hyaline, thin, occasionally extending beyond trichome, sometimes appearing wavy or lamellated. Trichomes with gliding motility, minutely constricted at crosswalls, occasionally constriction not evident, cylindrical, tapering slightly when conical end cell present, lacking necridia, 4.2–5.2 μm wide. Cells approximately isodiametric but can be longer or shorter than wide, blue-green, sometimes slightly yellow near apices, often granular, with thylakoids appearing distinctively fasciculated, 3.4–6.5 μm long. Apical cells bluntly rounded after hormogonia form, but becoming elongated and conical, yellowish in color, 3.6–5.2 μm wide, 4.2–9.4 μm long.

Holotype here designated: SBBG238514! Dried immobilized material prepared from the reference strain, SNI-TA29-BJ1.

Type locality: Thin incipient biocrust with algae and mosses from sample SNI-TA29 (Figure S1E), San Nicolas Island, Ventura County, California, 33.25362, –119.46002.

Etymology: L. *aeruginosus* = bright blue-green, named for the intense blue-green color of the trichomes.

Phylogenetic analysis

Based on 16S rRNA gene analysis (Figure 7), *Pycnacronema* forms a well-supported generic clade (0.91/50 BI posterior probability/ML bootstrap support) sister to *Symplocastrum. Microcoleus paludosus* SAG 1449-1a, *Parifilum solicrustae* SON57, *Pycnacronema flechtnerae*, and *Pycnacronema aeruginosum* all fall inside the *Pycnacronema* clade. *Microcoleus paludosus* is a classical taxon described in Gomont (1892) but known to not belong to the *Microcoleus* clade containing the type species, *M. vaginatus*. We are uncertain if strain SAG 1449-1a is an exact fit for *M. paludosus*, but if it is later confirmed to belong to that species, it will require that species to be transferred into *Pycnacronema*. *Parifilum solicrustae* is the type species of *Parifilum* and is clearly a later synonym of *Pycnacronema*. In the protologue for *Parifilum solicrustae*, Figure 2k–m is cited as the figure for the taxon, but Figure 2 is a phylogeny. Figure 3k–m has images of cyanobacteria, but the names are not given in the figure legend.

This is a problem for all the taxa described in Moreira-Fernandes et al. (2021), but can be considered a *lapsus calami*, and this type of error does not invalidate the taxa described. However, we correct the synonym here by making a new combination.

Pycnacronema solicrustae (Moreira-Fernandes, Girldo-Silva, D.Roush et Garcia-Pichel) Jusko et J.R.Johans., comb. nov.

Basionym: *Parifilum solicrustae* Moreira-Fernandes, Girldo-Silva, D.Roush et Garcia-Pichel. Coleofasciculaceae, a monophyletic home for the *Microcoleus steenstrupii* complex and other desiccation-tolerant filamentous cyanobacteria, 2021: 1577, Figure 3k–m.

Analysis of 16S–23S ITS rRNA region

Based on phylogenetic analysis of the 16S–23S ITS rRNA region (Figure 8), *Pycnacronema flechtnerae* and *P. aeruginosum* are distinct lineages from any of the previously described species. The species level nodes were highly supported in most cases. Both *P. aeruginosum* and *P. flechtnerae* had overall ITS rRNA region dissimilarity values >10% from other species, which is good evidence that both species are different lineages from each other and all other described species.

Analysis of ITS rRNA region secondary structures

There was significant variation in the ITS rRNA region secondary structures among all *Pycnacronema* species (Figure 9). All species shared a conserved basal clamp in the D1-D1' helix; however, variation in both size and sequence was observed in the terminal loop and other bulges along the helix. *Pycnacronema aeruginosum* was the most different from the others with a significantly longer stem and a 3-bp bulge before the terminal loop. Variation was observed among species in the Box-B helix as well. Differences in terminal loop sizes and sequences were observed. The structure of the Box-B helices of both *P. flechtnerae* and *P. aeruginosum* were unique to those taxa, and *P. aeruginosum* had a noncanonical U-G pairing near the terminal loop not observed in any other species. Perhaps, the most variation was observed in the V3 helix. Species varied in the number and size of bulges, at the terminal loops, noncanonical base pairings, and overall size of the helix. *Pycnacronema aeruginosum* had a notably shorter V3 helix than another other species at 36 base pairs. *Pycnacronema flechtnerae* differed from other species in the sequence of its terminal loop, as well as the presence of a bulge with one unpaired adenine on the upstream side of the terminal loop and three unpaired adenines on the downstream side. Differences in the ITS rRNA region secondary structures serve as good evidence of distinct lineages at the species level, suggesting the two new species are distinct from other *Pycnacronema* lineages.

One strain in *Pycnacronema* was further clarified by our molecular-based analyses. *Pycnacronema* sp. B-Tom (originally *Phormidium* sp. B-Tom, GenBank accessions EU196618, EU196672) was originally isolated from a sample collected from wet rocks 30 m from the Atlantic Ocean shore in Toninhas Beach, Ubatuba, municipality, São Paulo State, Brazil. The strain had trichomes (4.2)-5.5–6.3-(7.2) μm wide, cell length-width ratio 0.4–0.6, apical cell width (3.2)-4.5–5.8-(7.2) μm wide, apical cell length-width ratio 0.8–1.2, with conical end cells, which overlapped the dimensions of the reference strain of *Pycnacronema brasiliense*, although were slightly smaller in minimum and maximum size. The strain was sister to the *P. brasiliense* strains in the 16S rRNA gene phylogenetic analysis as well as the ITS rRNA region phylogenetic analyses (Figures 7 and 8). Furthermore, its 16S rRNA gene percent identity was 99.4% and its ITS rRNA region percent dissimilarity was 2.6% (Table S1), both thresholds satisfying the conclusion that it cannot be genetically separated from *P. brasiliense*. The secondary structures of the D1-D1', Box-B, and V3 helices were identical in the three *P. brasiliense* strains and *Pycnacronema* sp. B-Tom. *Pycnacronema brasiliense* was originally reported from wet rocks and the bark of trees in São José do Rio Preto, São Paulo State, Brazil. Thus, based on polyphasic analysis incorporating 16S rRNA gene and ITS rRNA region analysis, morphology, ecology, and biogeography, *Pycnacronema* sp. B-Tom appears to belong to *P. brasiliense*, and is so recorded in our phylogenies, ITS rRNA region figures, and tables. We have notified the authors of this sequence (A. Lokmer and J. Kaštovsky) of our conclusion, and they have offered to request the correction in GenBank.

Genus Konicacronema

Konicacronema protuberans Jusko et J.R. Johans. Figure 10

Filaments either solitary, entangled, or forming twisted bundles, without trichomes sharing a common sheath, 4.4–6.6 μm wide. Sheaths thin, hyaline, occasionally extending beyond trichome, sometimes not evident. Trichomes with gliding motility, distinctly constricted at crosswalls, cylindrical, tapering slightly at one to several terminal cells when conical end cell present, lacking necridia, 3.8–4.9 μm wide. Cells shorter than wide to isodiametric, blue-green in color, slightly yellow at crosswalls, granular, chromoplasm often restricted to parietal region of cell with thylakoids sometimes appearing fasciculated, 2.6–4.4 μm long. Apical cells bluntly rounded when hormogonia form but becoming bluntly to distinctly

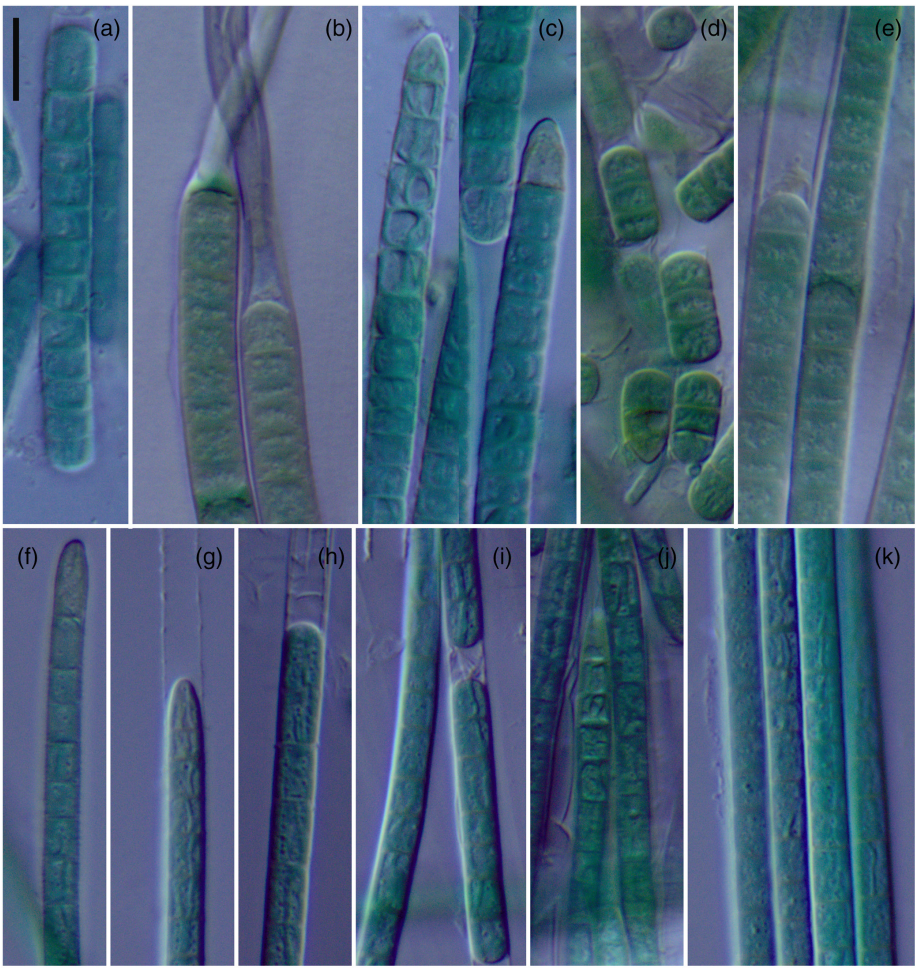

FIGURE 6 Micrographs of morphological features for species *Pycnacronema flechtnerae* and *P. aeruginosum*. Scale bar = 10 μm and applies to the entire figure. All photos are 1000× magnification. (a–e) *P. flechtnerae* SNI-TA3-BJ5. (f–k) *P. aeruginosum* SNI-TA29-BJ1. (Color figure can be viewed at wileyonlinelibrary.com). [Color figure can be viewed at wileyonlinelibrary.com]

conical, 3.0–4.6 μm wide, 3.6–11.2 μm long. Rare multiple *Kastovskya*-like protrusions sometimes form on the apical or penultimate cell in filament (Figure 10e).

Holotype here designated: SBBG238515! Dried immobilized material prepared from the reference strain, SNI-TA14-AZ4.

Paratypes here designated: SBBG238516!, SBBG238517!, Dried immobilized material prepared from the strains, SNI-TA6-AZ20 and SNI-TA17-BJ3, respectively.

Type locality: Well-developed rugose BSC from sample SNI-TA14, San Nicolas Island, Ventura County, California, 33.230516, –119.518651.

Etymology: L. *protuberans* = bulging. Named for the pseudopod-like protuberances on apical or subapical cells (Figure 10e).

Phylogenetic analysis

Based on 16S rRNA gene analysis (Figure 7), *Konicacronema* forms a well-supported (1.0/96 BI posterior probability/ML bootstrap support) generic clade, although containing strains *Trichocoleus sociatus* SAG 26 92 and *Funiculus tenuis* HSN023. *Trichocoleus sociatus* is a validly described taxon but is outside of the *Trichocoleus* clade, most likely containing the type species, which is not yet sequenced (Mühlsteinová et al., 2014). It was transferred to *Funiculus sociatus* by Moreira-Fernandes et al. (2021). However, *Funiculus* is clearly a later synonym of *Konicacronema* (Machado de Lima & Branco, 2020), and consequently both *T. sociatus* and *F. tenuis* require transfer to *Konicacronema*. The 16S rRNA gene analysis produced a well-supported (0.9, 89: BI, ML) species level clade consisting of all three *K. protuberans* strains serving as evidence of a lineage unique from the type species and *T. sociatus* SAG 26.92, with all three species having <98.8% identity in the 16S rRNA gene. *Funiculus tenuis* is more problematic, having 99.3%–99.4% identity with *K. protuberans*. Unfortunately, the 16S–23S ITS rRNA region has not been sequenced for *F. tenuis*, so definitive evidence that it is a separate lineage from our species is unavailable. The two species

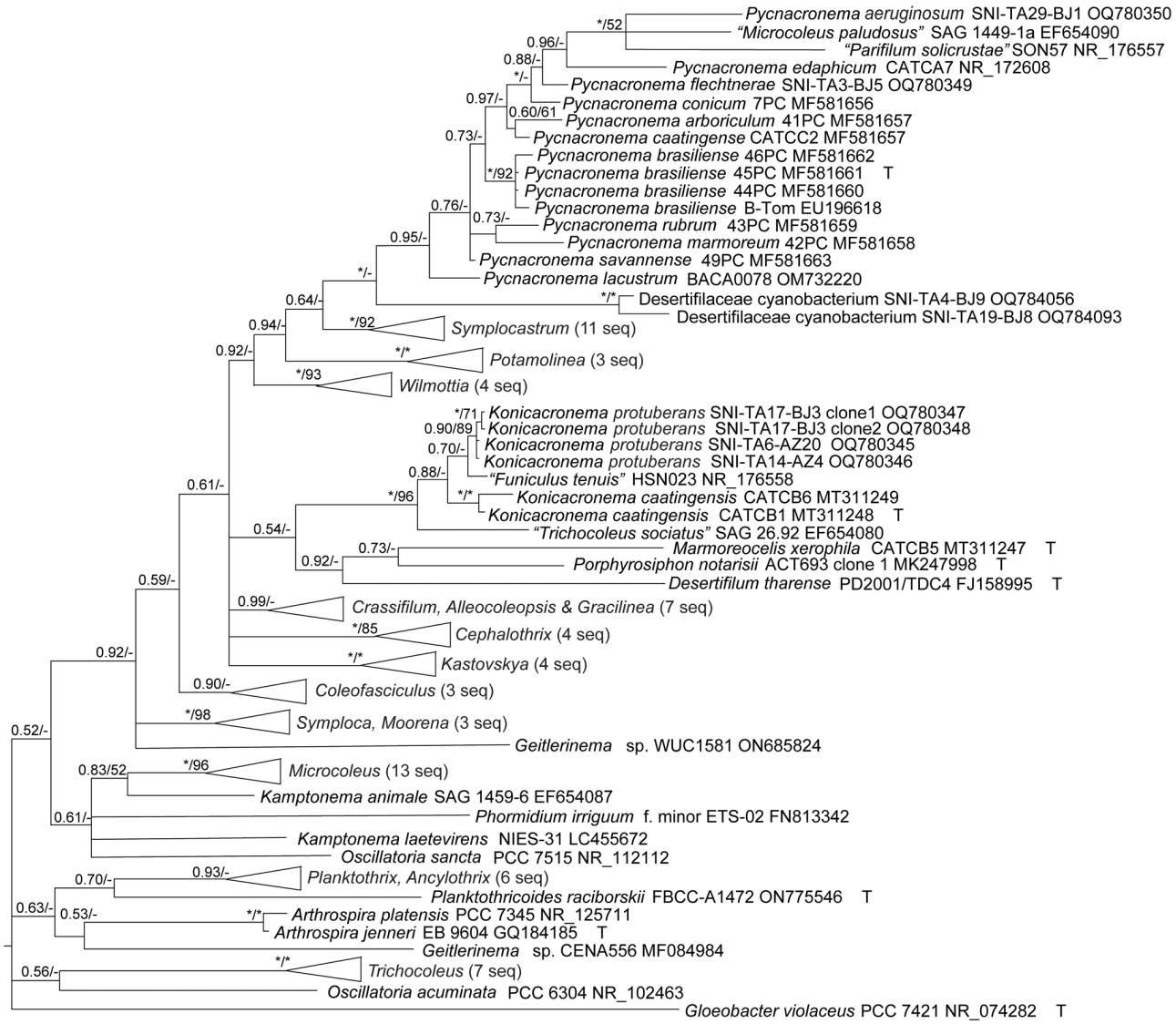

FIGURE 7 Bayesian inference phylogenetic tree for *Pycnacronema*, *Konicacronema*, and closely related genera. Maximum likelihood bootstrap support values were added to the nodes. "*" indicates full support for nodes (1.0 posterior probability, 100 bootstrap support). "-" indicates bootstrap support <50. All available *Pycnacronema* and *Konicacronema* 16S rRNA gene sequences were used from San Nicholas Island strains and those from previously described species in both genera.

are morphologically similar, but ecologically separated by climate and biogeography (*Funiculus tenuis* was found in soil crusts in the Great Basin Desert.). We conclude these are different species, but characterization of the ITS rRNA region in *F. tenuis* could lead to synonymization of the two species.

Konicacronema tenuis (Moreira-Fernandes, Giraldo-Silva, D.Roush & Garcia-Pichel) Jusko et J.R.Johans., comb. nov.

Basionym: *Funiculus tenuis* Moreira-Fernandes, Giraldo-Silva, D.Roush & Garcia-Pichel. Coleofasciculaceae, a monophyletic home for the *Microcoleus steenstrupii* complex and other desiccation-tolerant filamentous cyanobacteria, 2021: 1575, Figure 3n–p.

Konicacronema sociatus (West et G.S.West) Jusko et J.R.Johans., comb. nov.

Basionym: *Microcoleus sociatus* West et G.S. West. Welwitsch's African freshwater algae. 1897: 272, (no figure given).

Analysis of 16S–23S ITS rRNA region and secondary structures

All strains of *Konicacronema protuberans* were >11.8% dissimilar from *K. caatingense*, which serves as good evidence that the lineage is distinct from the type species. Additionally, variation was observed in the secondary ITS rRNA region structures between the type species and *K. protuberans* (Figure 11). The D1-D1' terminal loops varied significantly in size, with 11 and 4 base pairs, respectively. *K. protuberans* also showed

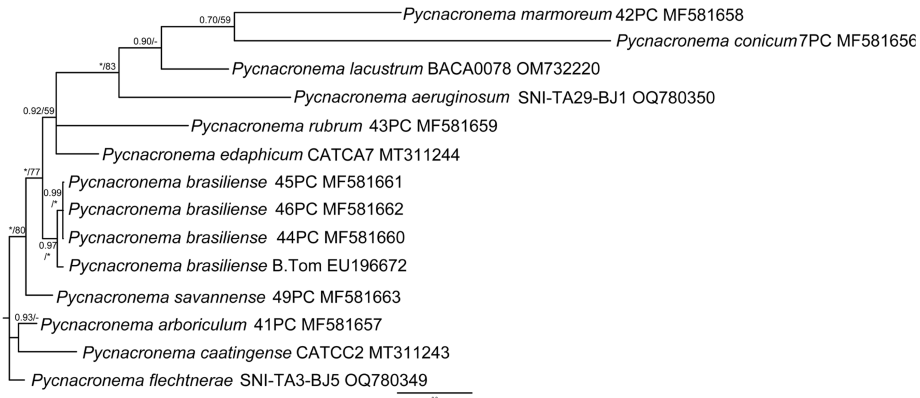

FIGURE 8 Maximum parsimony phylogeny based on *Pycnacronema* 16S–23S ITS rRNA region sequences with Bayesian inference posterior probability values added to the nodes. Sequences from previously described species and those from *P. flechtnerae* and *P. aeruginosum* were included in the analysis.

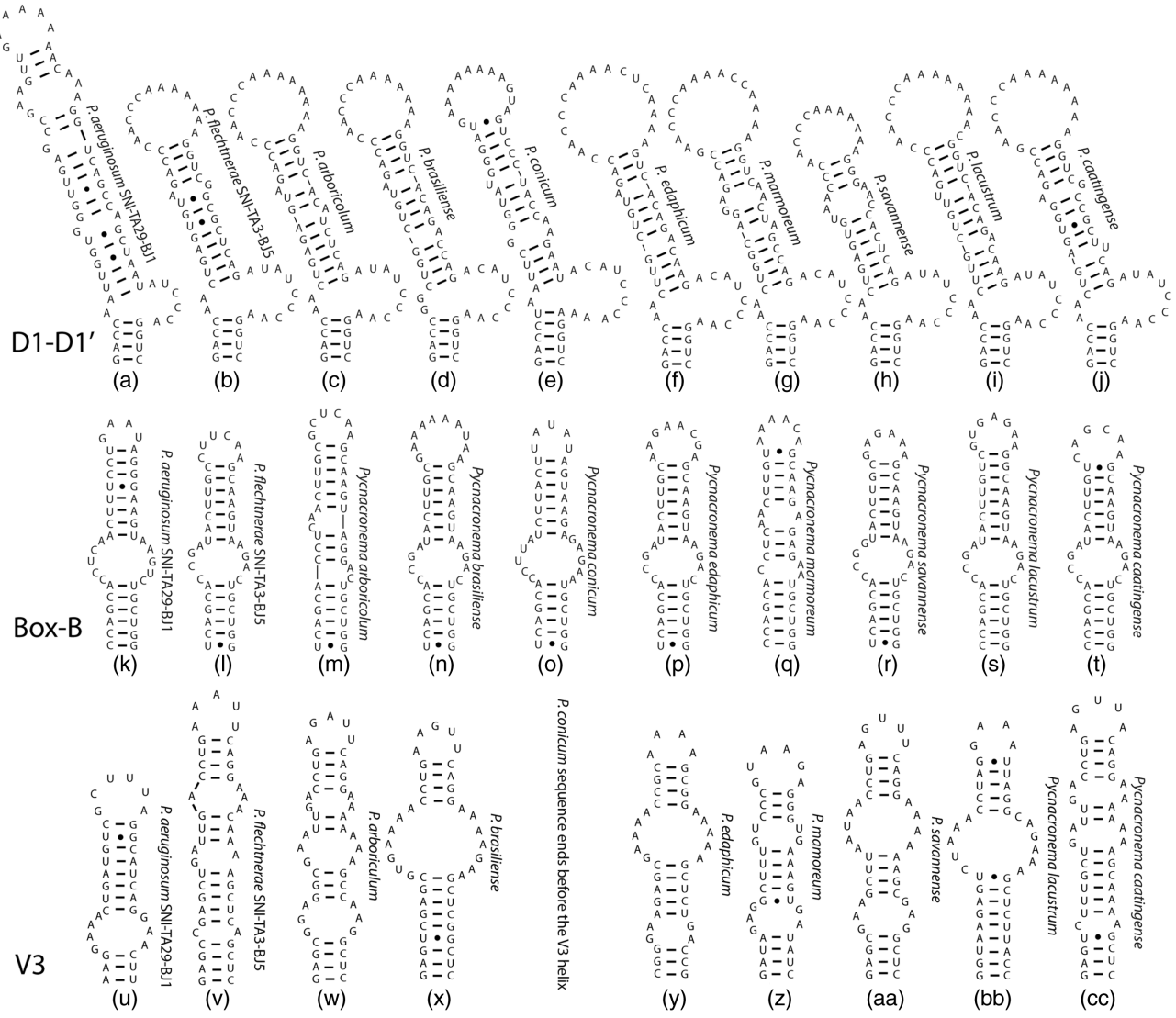

FIGURE 9 Hypothetical secondary ITS structures for the D1-D1', Box-B, and V3 helices in previously described *Pycnacronema* species, as well as *P. flechtnerae* and *P. aeruginosum*. (a–j) D1-D1' helix structures. (k–t): Box-B helix structures. (u-cc): V3 helix structures. The species for which each helix represents are included in the figure.

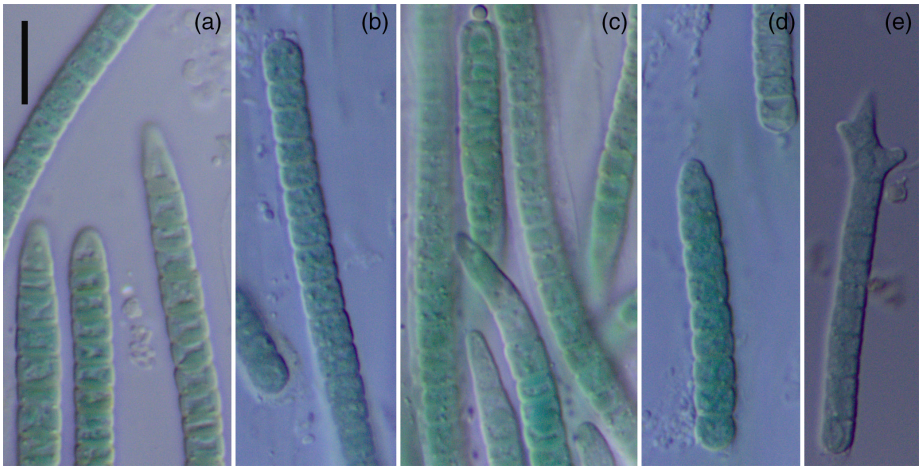

FIGURE 10 Photographs of diagnostic morphological features for species *Konicacronema protuberans* (Scale bar = 10 μm, applies to entire figure). (a–d) Strain SNI-TA14-AZ4. (e) SNI-TA6-AZ20 showing diagnostic *Kastovskya*-like protruberances in (e). [Color figure can be viewed at wileyonlinelibrary.com]

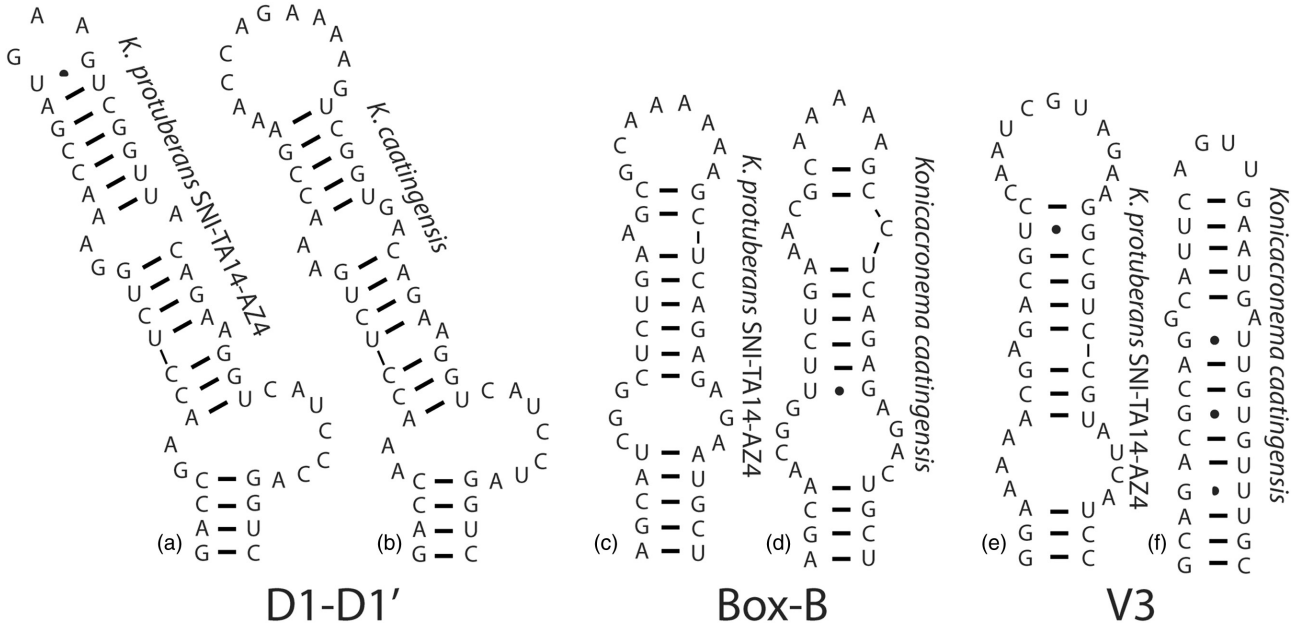

FIGURE 11 Hypothetical secondary ITS structures for the D1-D1', Box-B, and V3 helices in *Konicacronema protuberans* and the type species of the genus, *K. caatingense*. (a, b) D1-D1' structures. (c, d) Box-B structures. (e–f) V3 structures.

a U-G pairing directly before the terminal loop that was not observed in the type species. Significant variation was also observed in the Box-B and V3 helices terminal loops and presence of U-G pairings between the species.

DISCUSSION

The use of a polyphasic approach (Johansen & Cassamata, 2005; Mühlsteinová et al., 2014) to cyanobacterial taxonomy continues to be important for determining lineages worthy of taxonomic recognition. The use of morphological, ecological, and molecular characteristics for species delineation were integral to developing holistic arguments for species recognition in this study. The use of 16S rRNA gene identity thresholds for prokaryotic taxonomy has been shown to be inadequate as the sole criterion for species diagnosis due to insufficient variability in this region (Fox,et al., 1992), and this is highlighted especially in the case of *Atlanticothrix*. High 16S rRNA gene identity among species (and thus reduced taxonomic utility of the gene) has shown to be especially prevalent in the Nostocaceae across multiple studies, and *Atlanticothrix* is consistent with this trend (Bohunická et al., 2015; Casamatta et al., 2006; Johansen et al., 2014; Kaštovský et al., 2014; Řeháková et al., 2014). Although

none of the three described species meet the <98.7% 16S rRNA gene identity threshold historically used to differentiate prokaryotic species, there are repeatable, diagnosable morphological characteristics that may demonstrate lineage differentiation. The formation of *Nostoc*-like colonies in *A. nostocoides* (never observed in other species), along with variation in vegetative cell, heterocyte, and akinete size and shape among species, suggests that these groups are unique and could be confidently re-identified at the species level should they be isolated again in the future. Morphological evidence is strongly corroborated by differences in the ITS rRNA region, with species being >8% dissimilar in this region and varying in their secondary structures. The ITS rRNA region, unlike the 16S rRNA gene, is highly conserved at the species level but can vary significantly among closely related species at the genus level (Boyer et al., 2001, 2002; Johansen et al., 2011). The V2 helices are especially informative in this case, as they vary significantly among species but do not vary significantly within species. Additionally, biogeographical and ecological considerations serve as further evidence of unique lineages. The type species, *A. silvestris*, was originally isolated from tree leaves in the Atlantic Forest in Brazil, a habitat significantly different from the biocrusts found on San Nicolas Island, and is separated geographically from SNI by several thousand kilometers. Because these datasets are aligned, the total evidence is strong that the three new species are cohesive lineages separate from each other and also from *A. silvestris*.

In the case of *Pycnacronema* and *Konicacronema*, the genetic evidence more strongly suggests that the new species are distinct from all previously described species. The new species range from 10.4% to 27.2% overall dissimilarity in the ITS rRNA region, which is significantly higher than the 7% threshold, suggesting very strong evidence that they represent lineages worthy of taxonomic recognition (Erwin & Thacker, 2008; Pietrasiak et al., 2014, 2019; Osorio-Santos et al., 2014). Again, the ITS rRNA region is conserved at the species level but varies significantly among members of a genus, and both congeneric groups show significant differences in this area in sequence and secondary structure. The species in these two genera are morphologically very similar to previously described species but show ecological differences in substrate and climate. For example, *Pycnacronema* species have been described from tropical and subtropical climates on tree bark, wet rocks, and tropical soils. *Konicaronema caatingense* is from arid land biocrusts, but the caatinga is climatically very different from the temperate maritime climate on San Nicolas Island.

The presence on San Nicolas Island of species in multiple genera originally described from Brazil raises questions about the distribution of closely related taxa and the vectors responsible for their dispersal. Our current concept of species is tied to evolutionary processes and history, and it is understood that selection and evolution operates at the species level. Genera are a convenient way to group species, and it is recognized that genera may have less biological meaning than species. However, genera defined using molecular phylogeny do reflect the history of species lineages, so examining patterns of distribution of genera may be informative.

Whereas microbes in aquatic environments have numerous potential distribution vectors, such as waterfowl, water currents, and watercraft, terrestrial algae are generally limited to wind as a significant driver of dispersal (Marshall & Chalmers, 2006). Cyanobacteria have been found in atmospheric collections (Després et al., 2012), and it has been shown that BSCs can become eroded such that they can become aerosolized and then be carried by wind currents (Büdel et al., 2004). There are no wind patterns known that move from Brazil in the Southern Hemisphere to California in the Northern Hemisphere. However, episodic strong winds are known to move dust from Northern Africa (the Sahara Desert) to both the southern and northern hemispheres in the Americas. Particles originating from this region have been detected in both North America and the Amazon in appreciable numbers (Engelstaedter et al., 2006; Prospero et al., 2021). Although the three genera in this paper have not been isolated in Africa, it would be unsurprising if they were in future studies. With further investigation, it is probable that more overlap will be found between genera found in North and South America, and possibly Africa. Among the cyanobacteria in general, there is a phenomenon of hemispherically restricted species (Mühlsteinová et al., 2014; Pietrasiak et al., 2014, 2019), with rare exceptions potentially resulting from human vectoring (Hentschke et al., 2017). However, congeneric species may be widely distributed in respective hemispheres. This again may be a consequence of global wind patterns that are in most cases unlikely to carry microbial organisms across the equator due to the Coriolis Effect.

While it is unclear when the Brazilian and San Nicolas Island *Atlanticothrix*, *Pycnacronema*, and *Konicacronema* species last shared a common ancestor, the genetic and morphological divergence among them suggests evolutionarily significant time has passed since the lineage was cohesive. This provides further evidence that species of terrestrial algae (especially in BSCs) disperse infrequently regardless of which vectors are responsible for their distribution, and that cosmopolitan distributions in these taxa are unlikely. Future floristic studies on San Nicholas Island and elsewhere need to be undertaken to understand the full extent of cyanobacterial diversity, and thus to better understand distributional patterns. Although the taxa in this study come from environments with some overlapping attributes, it is likely that sampling bias (to some extent) has played a role in the

apparent distribution of these taxa. In recent years, a significant number of taxa have been described form Brazil due to a concerted effort by researchers (Alvarenga et al., 2021; Machado de Lima & Branco, 2020; Martins et al., 2018), and it is possible that this has led to the assumption that the region is particularly diverse. Although it is likely that Brazil is diverse given its size and wide range of environmental conditions, other regions across the globe remain under sampled due to lack of funding and researchers in the field. Further sampling efforts in understudied and underfunded regions are necessary to make this determination.

AUTHOR CONTRIBUTIONS

Brian M. Jusko: Data curation (lead); formal analysis (equal); investigation (lead); writing – original draft (lead); writing – review and editing (lead). **Jeffrey R. Johansen:** Conceptualization (equal); formal analysis (supporting); funding acquisition (lead); investigation (supporting); project administration (lead); resources (lead); supervision (lead); writing – review and editing (supporting).

ACKNOWLEDGMENTS

This work was funded by a subcontract from the Santa Barbara Botanical Garden with funding from U.S. Navy Cooperative Agreement Number N62473-21-2-0002. William Hoyer and Kristen Lehman assisted in collection of the soil samples. John Carroll University provided salary for both authors. Faculty and students at John Carroll University provided advice, training, and support, and we thank in particular Chris Sheil, Rebecca Drenovsky, Amanda Szinte, Mathew Luknis, and Salvadore Peron. Undergraduate students Mathew Luknis and Anastasia Zhydan assisted in isolation of strains reported in this study. Jan Kaštovský provided site data and dimensions for the *Pycnacronema brasiliense* B-Tom strain discussed in this manuscript.

ORCID

Jeffrey R. Johansen https://orcid.org/0000-0002-0794-9417

REFERENCES

Alvarenga, D. O., Andreote, A. P. D., Branco, L. H. Z., Delbaje, E., Cruz, R. B., de Mello Varani, A., & Fiore, M. F. (2021). *Amazonocrinis nigriterrae* gen. nov., sp. nov., *Atlanticothrix silvestris* gen. nov., sp. nov. and *Denronalium phyllosphericum* gen. nov., nostocacean cyanobacteria from Brazilian environments. *International Journal of Systematic and Evolutionary Microbiology*, *71*, 1–12. https://doi.org/10.1099/ijsem.0.00481

Baldarelli, L. M., Pietrasiak, N., Osorio-Santos, K., & Johansen, J. R. (2022). *Mojavia aguilerae* and *M. dolomitestris* – two new nostocaceae (Cyanobacteria) species from the Americas. *Journal of Phycology*, *58*, 502–516. https://doi.org/10.1111/jpy.13275

Becerra-Absalón, I., Johansen, J. R., Muñoz-Martín, M. A., & Montejano, G. (2018). *Chroakolemma* gen. nov. (Leptolyngbyaceae, Cyanobacteria) from soil biocrusts in the semi-desert Central Region of Mexico. *Phytotaxa*, *367*, 201–218. https://doi.org/10.11646/phytotaxa.367.3.1

Becerra-Absalón, I., Johansen, J. R., Osorio-Santos, K., & Montejano, G. (2020). Two new *Oculatella* (Oculatellaceae, Cyanobacteria) species in soil crusts from tropical semi-arid uplands of Mexico. *Fottea*, *20*, 160–170. https://doi.org/10.5507/fot.2020.010

Becking, L. G. M. B. (1934). Geobiologie of inleiding tot de milieukunde (No. 18-19). WP Van Stockum & Zoon.

Belnap, J. (2003). The world at your feet: Desert soil crusts. *Frontiers in Ecology and the Environment*, *1*, 181–189. https://doi.org/10.1890/1540-9295(2003)001[0181:TWAYFD]2.0.CO;2

Bohunická, M., Pietrasiak, N., Johansen, J. R., Gómez, E. B., Hauer, T., Gaysina, L. A., & Lukešová, A. (2015). *Roholtiella*, gen. nov. (Nostocales, Cyanobacteria)—a tapering and branching cyanobacteria of the family Nostocaceae. *Phytotaxa*, *197*(2), 84. https://doi.org/10.11646/phytotaxa.197.2.2

Boyer, S. L., Flechtner, V. R., & Johansen, J. R. (2001). Is the 16S–23S internal transcribed spacer region a good tool for use in molecular systematics and population genetics? A case study in cyanobacteria. *Molecular Biology and Evolution*, *18*, 1057–1069. https://doi.org/10.1093/oxfordjournals.molbev.a003877

Boyer, S. L., Johansen, J. R., Flechtner, V. R., & Howard, G. L. (2002). Phylogeny and genetic variance in terrestrial *Microcoleus* (Cyanophyceae) species based on sequence analysis of the 16S rRNA gene and associated 16S–23S ITS region. *Journal of Phycology*, *38*, 1222–1235. https://doi.org/10.1046/j.1529-8817.2002.01168.x

Brown, I., Tringe, S. G., Ivanova, N., Goodwin, L., Shapiro, N., Alcorta, J., Pan, D., Chrisstoserdov, A., Sarkisova, S., & Woyke, T. (2021). High-quality draft genome sequence of the siderophilic and thermophilic *Leptolyngbyaceae* cyanobacterium JSC-12. *Microbiology Resource Announcements*, *10*, e0049521. https://doi.org/10.1128/mra.00495-21

Büdel, B., Weber, B., Kühl, M., Pfanz, H., Sültemeyer, D., & Wessels, D. (2004). Reshaping of sandstone surfaces by cryptoendolithic cyanobacteria: bioalkalization causes chemical weathering in arid landscapes. *Geobiology*, *2*(4), 261–268. https://doi.org/10.1111/j.1472-4677.2004.00040.x

Carmichael, W. (1986). Isolation, culture, and toxicity testing of toxic freshwater cyanobacteria (blue-green algae). In V. Shilor (Ed.), *Fundamental research in homogenous catalysis* (Vol. 3, pp. 1249–1262). Gordon & Breach Publ.

Casamatta, D. A., Gomez, S. R., & Johansen, J. R. (2006). *Rexia erecta* gen. et sp. nov. and *Capsosira lowei* sp. nov., two newly described cyanobacterial taxa from the Great Smoky Mountain National Park (USA). *Hydrobiologia*, *561*, 13–26. https://doi.org/10.1007/s10750-005-1602-6

Després, V. R., Huffman, J. A., Burrows, S. M., Hoose, C., Safatov, A. S., Buryak, G., Fröhlich-Nowoisky, J., Elbert, W., Andreae, M. O., Pöschl, U., & Jaenicke, R. (2012). Primary biological aerosol particles in the atmosphere: a review. *Tellus B: Chemical and Physical Meteorology*, *64*(1), 15598. https://doi.org/10.3402/tellusb.v64i0.15598

Drummond, A. J., Ho, S. Y. W., Phillips, M. J., & Rambaut, A. (2006). Relaxed phylogenetics and dating with confidence. *PLoS Biology*, *4*, e88. https://doi.org/10.1371/journal.pbio.0040088

Dvořák, P., Hašler, P., & Poulíčková, A. (2012). Phylogeography of the *Microcoleus vaginatus* (Cyanobacteria) form three continents – a spatial and temporal characterization. *PLoS ONE*, *7*, e40153. https://doi.org/10.1371/journal.pone.0040153

Engelstaedter, S., Tegen, I., & Washington, R. (2006). North African dust emissions and transport. *Earth-Science Reviews*, *76*, 73–100. https://doi.org/10.1016/j.earscirev.2006.06.004

Erwin, P., & Thacker, R. (2008). Cryptic diversity of the symbiotic cyanobacterium *Synechococcus spongiarium* among sponge hosts. *Molecular Ecology*, *17*, 2937–2947. https://doi.org/10.1111/j.1365-294X.2008.03808.x

Evans, R. D., & Johansen, J. R. (1999). Microbiotic crusts and ecosystem processes. *Critical Reviews in Plant Sciences*, *18*, 183–225. https://doi.org/10.1080/07352689991309199

Flechtner, V. R., Boyer, S. L., Johansen, J. R., & DeNoble, M. L. (2002). *Spirirestis rafaelensis* gen.et sp. nov. (Cyanophyceae), a new cyanobacterial genus from arid soils. *Nova Hedwigia*, *74*, 1–24. https://doi.org/10.1127/0029-5035/2002/0074-0001

Flechtner, V. R., Johansen, J. R., & Belnap, J. (2008). The biological soil crusts of the San Nicholas Island: Enigmatic algae from a geographically isolated ecosystem. *Western North American Naturalist*, *68*, 405–436. https://doi.org/10.3398/1527-0904-68.4.405

Fox, G. E., Wisotzkey, J. D., & Jurtshuk, P. (1992). How close is close: 16S rRNA sequence identity may not be sufficient to guarantee species identity. *International Journal of Systematic Bacteriology*, *42*(1), 166–170. https://doi.org/10.1099/00207713-42-1-166

Gelman, A., & Rubin, D. B. (1992). Inference from iterative simulation using multiple sequences. *Statistical Science*, *7*, 157–511. https://doi.org/10.1214/ss/1177011136

Gomont, M. (1892). Monographie des Oscillariées (Nostocacées Homocystées). Deuxième partie. - Lyngbyées. *Annales des Sciences Naturelles, Botanique*, Série 7, *16*, 91–264, pls 1–7.

Harper, K. T., & Marble, J. R. (1989). Effect of timing of grazing on soil-surface cryptogamic communities in a Great Basin low-shrub desert: A preliminary report. *Great Basin Naturalist*, *49*, 104–107.

Hentschke, G. S., Johansen, J. R., Pietrasiak, N., Rigonato, J., Firoe, M. F., & Sant'Anna, C. L. (2017). *Komarekiella atlantica* gen. et sp. nov. (Nostocaceae, Cyanobacteria): A new subaerial taxon from the Atlantic Rainforest and Kauai, Hawaii. *Fottea*, *17*, 178–190.

Jeffries, D. L., Link, S. O., & Klopatek, J. M. (1993). CO_2 fluxes of cryptogamic crusts. I. Response to resaturation. *New Phytologist*, *125*, 163–173. https://doi.org/10.1111/j.1469-8137.1993.tb03874.x

Johansen, J. R., Bohunická, M., Lukešová, A., Hrčková, K., Vaccarino, M. A., & Chesarino, N. M. (2014). Morphological and molecular characterization within 26 strains of the genus *Cylindrospermum* (Nostocaceae, Cyanobacteria), with descriptions of three new species. *Journal of Phycology*, *50*, 187–202. https://doi.org/10.1111/jpy.12150

Johansen, J. R., & Cassamata, D. A. (2005). Recognizing cyanobacterial diversity through the adoption of a new species paradigm. *Algological Studies*, *117*, 71–93. https://doi.org/10.1127/1864-1318/2005/0117-0071

Johansen, J. R., Kovacik, L., Casamatta, D. A., Fučíková, K., & Kaštovský, J. (2011). Utility of 16S-23S ITS sequence and secondary structure for recognition of intrageneric and intergeneric limits within cyanobacterial taxa: *Leptolyngbya corticola sp. nov.* (Pseudanabaenaceae, Cyanobacteria). *Nova Hedwigia*, *92*, 283–302. https://doi.org/10.1127/0029-5035/2011/0092-0283

Jung, P., Mikhailyuk, T., Emrich, D., Baumann, K., Dultz, S., & Büdel, B. (2020). Shifting boundaries: Ecological and geographical range expansion based on three new species in the cyanobacterial genera *Cyanocohniella*, *Oculatella*, and *Aliterella*. *Journal of Phycology*, *56*, 1216–1231. https://doi.org/10.1111/jpy.13025

Kaštovský, J., Berrendero Gomez, E., Hladil, J., & Johansen, J. R. (2014). *Cyanocohniella calida* gen. et sp. nov. (Cyanobacteria: Aphanizomenonaceae) a new cyanobacterium from the thermal springs from Karlovy Vary, Czech Republic. *Phytotaxa*, *181*, 279–292. https://doi.org/10.11646/phytotaxa.181.5.3

Kaštovský, J., Johansen, J. R., Hauerová, R., & Akagha, M. U. (2023). Hot is rich—An enormous diversity of simple trichal cyanobacteria from Yellowstone hot springs. *Diversity*, *15*, 975. https://doi.org/10.3390/d15090975

Kleiner, E. F., & Harper, K. T. (1972). Environment and community organization in the grasslands of Canyonlands National Park. *Ecology*, *53*, 299–309. https://doi.org/10.2307/1934086

Larkin, M. A., Blackshields, G., Brown, N. P., Chenna, R., McGettigan, P. A., McWilliam, H., Valentin, F., Wallace, I. M., Wilm, A., Lopez, R., Thompson, J. D., Gibsin, T. J., & Higgins, D. G. (2007). Clustal W and Clustal X version 2.0. *Bioinformatics*, *23*, 2947–2948. https://doi.org/10.1093/bioinformatics/btm404

Luz, R., Cordeiro, R., Kaštovský, J., Johansen, J. R., Dias, E., Fonseca, A., Urbatzka, R., Vasconcelos, V., & Gonçalves, V. (2023). Description of four new filamentous cyanobacterial taxa from freshwater habitats in the Azores Archipelago. *Journal of Phycology*, *2023*, 1–16. https://doi.org/10.1111/jpy.13396

Machado de Lima, N. M., & Branco, L. H. Z. (2020). Biological soil crusts: New genera and species of cyanobacteria from Brazilian semi-arid regions. *Phytotaxa*, *470*, 263–281. https://doi.org/10.11646/PHYTOTAXA.470.4.1

Marshall, W. A., & Chalmers, M. O. (2006). Airborne dispersal of Antarctic terrestrial algae and cyanobacteria. *Ecography*, *20*, 585–594. https://doi.org/10.1111/j.1600-0587.1997.tb00427.x

Martins, M. D., Machado-de-Lima, N. M., & Branco, L. H. Z. (2018). Polyphasic approach using multilocus analyses supports the establishment of the new aerophytic cyanobacterial genus *Pycnacronema* (Coleofacisculaceae, Oscillatoriales). *Journal of Phycology*, *55*, 146–159. https://doi.org/10.1111/jpy.12805

Mesfin, M., Johansen, J. R., Pietrasiakl, N., & Baldarelli, L. M. (2020). *Nostoc oromo* sp. nov. (Nostocales, Cyanophyceae) from Ethiopia: a new species based on morphological and molecular evidence. *Phytotaxa*, *433*(2), 81–93. https://doi.org/10.11646/phytotaxa.433.2.1

Miller, M. A., Pfeiffer, W., & Schwartz, T. (2010). Creating the CIPRES Science Gateway for inference of large phylogenetic trees. In 2010 gateway computing environments workshop (GCE) (pp. 1–8).

Moreira-Fernandes, V., Giraldo-Silva, A., Roush, D., & Garcia-Pichel, F. (2021). Coleofasciculaceae, a monophyletic home for the *Microcoleus steenstrupii* complex and other desiccation-tolerant filamentous cyanobacteria. *Journal of Phycology*, *57*, 1563–1579. https://doi.org/10.1111/jpy.13199

Mühlsteinová, R., Johansen, J. R., Pietrasiak, N., Martin, M. P., Osorio-Santos, K., & Warren, S. D. (2014). Polyphasic characterization of *Trichocoleus desertorum* sp. nov. (Pseudanabaenales, Cyanobacteria) from desert soils and phylogenetic placement of the genus *Trichocoleus*. *Phytotaxa*, *163*, 241–261. https://doi.org/10.11646/phytotaxa.163.5.1

Nübel, U., Garcia-Pichel, F., & Muyzer, G. (1997). PCR primers to amplify 16S rRNA genes from cyanobacteria. *Applied and Environmental Microbiology*, *63*, 3327–3332. https://doi.org/10.1128/aem.63.8.3327-3332.1997

Osorio-Santos, K., Pietrasiak, N., Bohunická, M., Miscoe, L. H., Kováčik, L., Martin, M. P., & Johansen, J. R. (2014). Seven new species of *Oculatella* (Pseudanabaenales, Cyanobacteria): Taxonomically recognizing cryptic diversification. *European Journal of Phycology*, *49*, 450–470. https://doi.org/10.1080/09670262.2014.976843

Pietrasiak, N., Mühlsteinová, R., Siegesmund, M., & Johansen, J. R. (2014). Phylogenetic placement of *Symplocastrum* (Phormidiaceae, Cyanobacteria) with description of two new species: *S. flechtnerae* and *S. torsivum*. *Phycologia*, *53*, 529–541. https://doi.org/10.2216/14-029.1

Pietrasiak, N., Osorio-Santos, K., Shalygin, S., Martin, M. P., & Johansen, J. R. (2019). When is a lineage a species? A case study in *Myxacorys* gen. nov. (Synechococcales: Cyanobacteria) with the description of two new species from the Americas. *Journal of Phycology*, *55*, 976–996. https://doi.org/10.1111/jpy.12897

Pietrasiak, N., Reeve, S., Osorio-Santos, K., Lipson, D. A., & Johansen, J. R. (2021). *Trichotorquatus* gen. nov. — A new genus of soil cyanobacteria from American drylands. *Journal of Phycology*, *57*, 886–902. https://doi.org/10.1111/jpy.13147

Prospero, J. M., Delany, A. C., Delany, A. C., & Carlson, T. N. (2021). The discovery of African dust transport to the Western Hemisphere and the Saharan air layer: A history. *Bulletin of the American Meteorological Society*, *102*(6), e1239–e1260. https://doi.org/10.1175/BAMS-D-19-0309.1

Rambaut, A. (2009). *FigTree*, (version) 1.4.3. http://tree.bio.ed.ac.uk/software/figtree.

Řeháková, K., Johansen, J. R., Casamatta, D. A., Xuesong, L., & Vincent, J. (2007). Morphological and molecular characterization of selected desert soil cyanobacteria: Three species new to science including *Mojavia pulchra* gen. et sp. nov. *Phycologia*, *45*, 481–502. https://doi.org/10.2216/06-92.1

Řeháková, K., Mareš, J., Lukešová, A., Zapomělová, E., Bernardová, K., & Hrouzek, P. (2014). *Nodularia* (Cyanobacteria, Nostocaceae): A phylogenetically uniform genus with variable phenotypes. *Phytotaxa*, *172*, 235–246. https://doi.org/10.11646/phytotaxa.172.3.4

Ronquist, F., Teslenko, M., Van Der Mark, P., Ayres, D. L., Darling, A., Hohna, S., Larget, B., Liu, L., Suchard, M. A., & Huelsenbeck, J. P. (2012). MrBayes 3.2, efficient Bayesian phylogenetic inference and model choice across a large model space. *Systematic Biology*, *61*, 539–542. https://doi.org/10.1093/sysbio/sys029

Shalygin, S., Shalygina, R. R., Redkina, V. V., Gargas, C. B., & Johansen, J. R. (2020). Description of *Stenomitos kolaenensis* and *S. hiloensis* sp. nov. (Leptolyngbyaceae, Cyanobacteria) with an emendation of the genus. *Phytotaxa*, *440*(2), 108–128. https://doi.org/10.11646/phytotaxa.440.2.3

Sherwood, A. R., Carlile, A. L., Vaccarino, M. A., & Johansen, J. R. (2015). Characterization of Hawaiian freshwater and terrestrial cyanobacteria reveals high diversity and numerous putative endemics. *Phycological Research*, *63*, 85–92. https://doi.org/10.1111/pre.12080

Stamatakis, A. (2014). RAxML version 8, a tool for phylogenetic analysis and post- analysis of large phylogenies. *Bioinformatics*, *30*, 1312–1313. https://doi.org/10.1093/bioinformatics/btu033

Strunecký, O., & Ivanova, A. P. (2023). An updated classification of cyanobacterial orders and families based on phylogenomic and polyphasic analysis. *Journal of Phycology*, *59*, 12–51. https://doi.org/10.1111/jpy.13304

Swofford, D. L. (1998). *PAUP*. Phylogenetic analysis using parsimony (*and other methods)*. Version 4.02b. Sinauer Associates.

Weber, B., Belnap, J., Büdel, B., Antoninka, A. J., Barger, N. N., Chaudhary, V. B., Darrouzet-Nardi, A., Eldridge, D. J., Faist, A. M., Ferrenberg, S., Havrilla, C. A., Huber-Sannwald, E., Issa, O. M., Maestre, F. T., Reed, S. C., Rodriguez-Caballero, E., Tucker, C., Young, K. E., Zhang, Y., … Bowker, M. A. (2022). What is a biocrust? A refined, contemporary definition for a broadening research community. *Biological Reviews*, *97*, 1768–1785. https://doi.org/10.1111/brv.12862

West, N. E. (1990). Structure and function of microphytic soil crusts in wildland ecosystems of arid to semiarid regions. *Advances in Ecological Research*, *20*, 179–223. https://doi.org/10.1016/S0065-2504(08)60055-0

West, W., & West, G. S. (1897). Welwitsch's African freshwater algae. *Journal of Botany, British and Foreign*, *35*, 1–7, 33–42, 77–89, 113–122, 172–183, 235–243, 264–272, 297–304, pls 365–369.

Wilmotte, A., Auwera, G. V. D., & Watcher, R. D. (1993). Structure of the 16S rRNA of the thermophilic cyanobacterium *Chlorogloeopsis* HTF ('Mastigocladus laminosus hTF') strain PCC7518, and phylogenetic analysis. *FEBS Letters*, *317*, 96–100. https://doi.org/10.1016/0014-5793(93)81499-P

Zuker, M. (2003). Mfold web server for nucleic acid folding and hybridization prediction. *Nucleic Acids Research*, *31*(13), 3406–3415. https://doi.org/10.1093/nar/gkg595

SUPPORTING INFORMATION

Additional supporting information can be found online in the Supporting Information section at the end of this article.

Figure S1. Examples of soil surface features in San Nicolas Island study sites. A. Site SNI-TA1, biocrust with lichens, mosses, and algal crust evident. B. Site SNI-TA5, uncrusted soil surface. C. Site SNI-TA26, rugose moss and cyanobacterial crust. D. Site SNI-TA23, exposed caliche. E. Site SNI-TA29, thin incipient crust with algae and mosses. F. Site SNI-TA17, early successional stage cyanobacterial crust.

Figure S2. Hypothetical ITS secondary structures for the D1-D1'. Box-B, and V3 helices for all strains representing Atlanticothrix crispata, A. testacea, A. nostocoides, and A. silvestris. A: Common D1-D1' helix for all strains representing A. crispata, A. testacea, and A. nostocoides except SNI-TA23-BJ35 operon 2. B: D1'D1' helix for A. crispata SNI-TA23-BJ35 operon 2. C: A. silvestris D1-D1'. D: Common Box-B helix among all A. testacea and A. nostocoides strains. E: Common Box-B helix for all A. crispata strains except SNI-TA23-BJ35 operon 2. F: Box-B helix for SNI-TA23-BJ35 operon 2. G: A. silvestris Box-B helix. H: Common V3 helix among all A. testacea and A. nostocoides strains. I: Common V3 helix for all A. crispata strains except SNI-TA23-BJ35 operon 2. J: V3 helix for SNI-TA23-BJ35 operon 2. K: A. silvestris V3 helix.

Figure S3. Principal component analysis based on Atlanticothrix strain cell measurements. Analysis was run on mean length and width measurements and length-width ratios for vegetative cells, apical cells, heterocytes, and akinetes. Each average measurement was obtained by taking 30 individual measurements for each cell length and width. Principal component axes 1 and 2 are displayed.

Table S1. Percent identity based on 16S rRNA gene sequence and percent dissimilarity based on 16S–23S ITS rRNA region sequence among Pycnacronema species. Percent identity in the 16S rRNA gene <98.7% is considered evidence of different species, Percent dissimilarity (PD) in the ITS rRNA region >7.0 is considered strong evidence of different species, while PD <3.0 is considered evidence of same species. Both threshold analyses confirm that the 10 described species of Pycnacronema are supported by molecular data and that the previously undesignated strain Pycnacronema sp. B-Tom belongs in P. brasiliense.

How to cite this article: Jusko, B. M., & Johansen, J. R. (2024). Description of six new cyanobacterial species from soil biocrusts on San Nicolas Island, California, in three genera previously restricted to Brazil. *Journal of Phycology*, *60*, 133–151. https://doi.org/10.1111/jpy.13411